High-resolution temperature and precipitation variability of southwest Anatolia since 1730 CE from Lake Gölcük sedimentary records

Iliya Bauchi DANLADI[1,*] ⓘ, **Sena AKÇER-ÖN[1]** ⓘ, **Z. Bora ÖN[1]** ⓘ, **Sabine SCHMIDT[2]** ⓘ
[1]Department of Geological Engineering, Faculty of Engineering, Muğla Sıtkı Koçman University, Muğla, Turkey
[2]CNRS, University Bordeaux, EPOC, EPHE, UMR 5805, Pessac, France

Abstract: We report high-resolution multiproxy analyses [lithology, µXRF and magnetic susceptibility (MS)] of two short gravity sediment cores from the crater Lake Gölcük, southwest Turkey. Our results provide a detailed hydroclimatic record for the last ~290 years. Aided with factor analysis of µXRF data and ^{210}Pb and ^{137}Cs dating, our multiproxy data show that the Lake Gölcük records documented a series of wet and dry periods between ~ 1730 (±71) and ~ 2018 (±3) CE. Wet periods are evidenced by dark olive green mixed lithology (sandy, clay, and silts) and high values in MS and log(Sr/Ca). On the other hand, dry periods are associated with light olive green clayey mud lithology and high values in log(Ca/K). We relate the wet periods to negative North Atlantic Oscillation (NAO−) and the dry periods to NAO+. Additionally, all wet periods are related with time of low solar activity and dry periods, except Dalton Minimum, are related with periods of high solar activity. Consequently, we suggest that hydroclimatic changes observed in the Lake Gölcük sedimentary records were caused by the influence of large-scale atmospheric circulation and solar activity.

Key words: Hydroclimate, paleoclimate, solar activity, North Atlantic Oscillation

1. Introduction

The Mediterranean region has been reported as one of the regions expected to be severely affected by current climate change, particularly drought (Giorgi, 2006; Lelieveld et al., 2012; Stocker et al., 2013). While most of these present-day climate extremes have been ascribed to human-induced climate disturbances (Stocker et al., 2013; Cook et al., 2016), the disruption of natural climate is not fully understood (Luterbacher et al., 2012). The knowledge of the extent to which, humans disrupt the natural system relies on our appreciation of paleoclimate changes. In turn, understanding the paleoclimate changes and the climate mechanisms that operate is of crucial significance not only for understanding today's climate but also for predicting future climatic changes.

Some recent paleoclimate studies in the Eastern Mediterranean (EM) suggest that the regional winter climate, to some extent, is linked to the North Atlantic Oscillation (NAO) (Luterbacher et al., 2012; Koutsodendris et al., 2017; Lüning et al., 2019). Estimated from the pressure difference between the subtropical high and subpolar low, the NAO is an index that is claimed to describe the changes of the large atmospheric circulation over the North Atlantic (Hurrell, 1995). These changes are usually related with changes in the jet stream and storm tracks which are then translated in temperature and precipitation changes. In the EM, the stronger (weaker) NAO is reported to be related to drier and cooler (wetter and warmer) climate conditions (Kahya, 2011). However, it has also been revealed in the literature that this may not always be the case as climate modes may change through time (Roberts et al., 2012; Cook et al., 2016). In Anatolia, other than the NAO (Türkeş and Erlat, 2009), the region is also under a possible influence of the North Sea-Caspian Pattern (NCP) during the winter (Kutiel et al., 2002).

In addition, the possible NCP influence has also been previously reported in some of the paleoclimate records of the Central (Lake Nar, Jones et al., 2006) and SW Anatolia (Lake Salda, Danladi and Akçer-Ön, 2018). Until recently, a number of paleoclimate studies have shown that solar variability is also a component of the climate change during the last millennium (Akçer Ön, 2017; Brahim et al., 2018; Danladi and Akçer-Ön, 2018; Kushnir and Stein, 2019; Wagner and Zorita, 2005; and references therein).

The present paper aims to contribute to a better understanding of the teleconnections responsible for past climate changes in the Anatolia by presenting continuous and high resolution multiproxy sedimentary records from the Lake Gölcük (SW Anatolia; Figure 1) covering the last ~290 years. The multiproxy in the current study comprises of lithological description, µXRF and magnetic susceptibility measurements. µXRF results were further evaluated using factor analysis, and the age-depth model was reconstructed through a Bayesian framework by using ^{210}Pb and ^{137}Cs dating. The current study also allows a direct comparison of the reconstructed climate changes with modern meteorological data. Furthermore, in order to understand the synchronicity and unravel the climate mechanisms during the study period, the Lake Gölcük record was compared with data from regional lake records, reconstructed NAO index and total solar irradiance data.

1.1. Study area

Located in the Isparta Province of SW Anatolia, the Lake Gölcük (37°43.756'N, 30°29.688'E) is a small crater lake, with an approximate surface area of 1.05 km² (Figure 1). The Lake Gölcük is a closed basin. The bathymetry map shows that the lake's deepest point is 37.28 m below lake level (DSİ, 1978; Figure 1). Isparta region is in a transitional location between
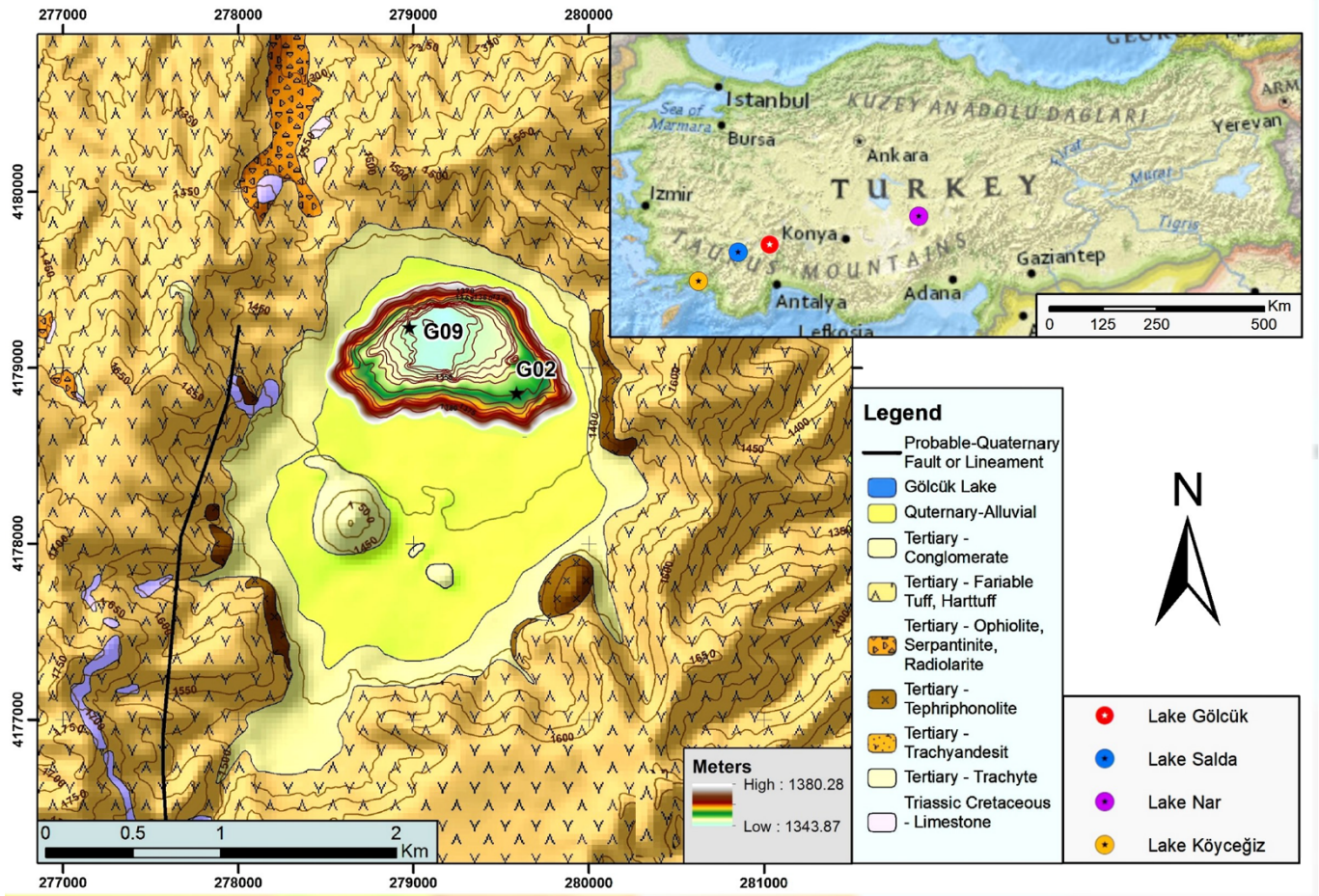
* Correspondence: iliyadbauchi@yahoo.com

Figure 1. Turkey map showing the Lake Gölcük and the lakes used for comparison (Lake Salda, Lake Köyceğiz, and Lake Nar). The geological units in the Lake Gölcük surroundings. Locations of core G02 and G09 have been indicated on the bathymetry map.

dry continental Anatolian and mild Mediterranean climate, which are characterized by mild to wet winters and dry summers. Average yearly temperature and precipitation for the period 1929–2019 were 12.2 °C and 570.2 mm, respectively.[1] Owing to peculiar fauna and flora in its environs (Japoshvili et al., 2010, 2017; Öztürk, 2017; Yavuz and Çobanoğlu, 2018), the Lake Gölcük was declared as a nature park by the Turkish Government in 1991.

The geomorphology of the Lake Gölcük region, which host various volcanic cones, domes, valleys, calderas and paleo calderas, has been described and mapped in the study of Cengiz et al. (2006) and Canpolat (2015). Today, the regional geology comprises of mainly Cenozoic aged volcanic materials (tuff, tephrophonolite, trachyandesite and conglomerates) with Quaternary alluvial sediments surrounding the lake (Figure 1). A probable Quaternary fault or lineament is located on the western part of the Lake (Cengiz et al., 2006).

2. Materials and methods

Two sediment cores (G02 and G09) were retrieved during the drilling campaign of a TÜBİTAK Project (No 117Y517) in September 2018. The coring locations were determined using a sonar device, which has the ability to reveal bathymetry and possible underlying lithology. The core sediments G02 (11 cm long, latitude: 37°43'44.32"N, longitude: 30°29'56.05"E) and G09 (15 cm long, latitude: 37°43'55.94"N, longitude: 30°29'33.73"E) were recovered from water depths of 15 m and 22.5 m, respectively. The cores were then split into two and lithologically defined.

2.1. Micro X-ray fluorescence (µXRF) analysis

µXRF analysis was carried out at the geochemistry laboratory of the İstanbul Technical University using Itrax µXRF scanner. The scanner is semiquantitatively capable of measuring wide spectrum elements (Croudace et al., 2006, 2019). The scanning measurements in this study were carried out at 1 mm interval. Thirty seconds scan time at 10 kV and 0.3 mA current were used during the measurements. Although, the µXRF scanner measured wide range of elements, only the elements with continuous measurements and high counts per second counts, which are Fe, Sr, Ca, Zr and K have been selected for the purpose of this study. The rationale behind choosing elements with continuous

measurements and high counts per second relies on the fact that they have been adequately measured.

2.1.1. Factor analysis

Factor analysis is one of the statistical approaches of extracting few explanatory controlling processes from a large set of data. However, the nature of µXRF counts is compositional and thus needs to be appropriately transformed before any statistical analysis (Weltje and Tjallingii, 2008). Furthermore, since factor analysis depends on the covariance matrix, extreme values or outliers in the data have serious influence on factor analysis results (Reimann et al., 2008). Therefore, our strategy is to follow the algorithm proposed by Filzmoser et al. (2009). They offer centered logratio transformation of the compositional data and use the methods of robust statistics, a subject of statistics that is more immune to the effect of the outliers. Unlike other proposed transformations for compositional data, centered logratio transformation treats the variables symmetrically and its results are interpretable. We apply principal factor analysis method through robCompositions package (Filzmoser et al., 2018) in R (R Core Team, 2020) to handle the algorithm explained above.

2.2. Magnetic susceptibility analysis

Magnetic susceptibility analysis was performed on core G02 and G09 at 1 mm intervals using a Bartington point sensor in Geotek Multi-Sensor Core Logger equipment in the EMCOL sedimentology laboratory of the İstanbul Technical University. The MSCL equipment is used to measure physical properties such as magnetic susceptibility (MS), porosity, density and water content in sediment cores (Weber et al., 1996). MS (SI) was measured and used for the purpose of this study.

2.3. Radionuclides

Activities of ^{210}Pb, ^{226}Ra and ^{137}Cs were measured in core G09 at the University of Bordeaux (France) using a high efficiency, well-type gamma spectrometer (Canberra, Toledo, OH, USA; Schmidt et al., 2014). Detector calibration was done using IAEA reference materials. The dating was established based on ^{210}Pb ($T_{1/2} = 22.3$ years), a widely used method to calculate sediment accumulation rates in sediments (Appleby, 2002). According to its half live, the method relies on the decrease of excess activity of ^{210}Pb ($^{210}Pb_{xs}$) with depth in sediments.

Excess ^{210}Pb ($^{210}Pb_{xs}$) was calculated by subtracting the measured ^{226}Ra activity, corresponding to the supported fraction, from the total ^{210}Pb activity in the sediment.

3. Results and interpretation

3.1. Dating

Profile of $^{210}Pb_{xs}$ activity in core G09 presents a classical trend with activities decreasing exponentially with depth to reach negligible values deeper to 7–8 cm (Table 1). The ^{210}Pb dating was checked using an independent time marker, the ^{137}Cs measured during the same gamma counting session. ^{137}Cs was detectable only in the top 5 cm of the core (Table 1; Figure 2). The occurrence of the artificial ^{137}Cs ($T_{1/2} = 30$ years) in the environment is primarily the result of the nuclear weapon test fallout, with a maximum fallout in 1963, and first detections in sediments early 1950s. The onset of ^{137}Cs around 1950 strengthens the ^{210}Pb dating.

3.1.1. Age model

Dating results are used to construct a Bayesian age-depth model through the rbacon package (Blaauw and Christen, 2011) in R (R Core Team, 2020). The prior couplet for the gamma distribution describing the accumulation rate is selected as $(\alpha,\beta) = (1.5,2)$ and the prior couplet for the beta distribution describing the memory of the accumulation is selected as $(\alpha,\beta) = (4,10/7)$ [for details of the model and prior selection see the rbacon package manual and Blaauw and Christen (2011)]. Since, the oldest dated point is at the 67.5 mm depth, the age model is extrapolated for the rest of the G09 (15 cm long) in rbacon. According to the age-depth model, G09 covers the time interval from 1730 to 2018 CE (Figure 2).

Table 1. Dating of core G09 based on ^{137}Cs and $^{210}Pb_{xs}$.

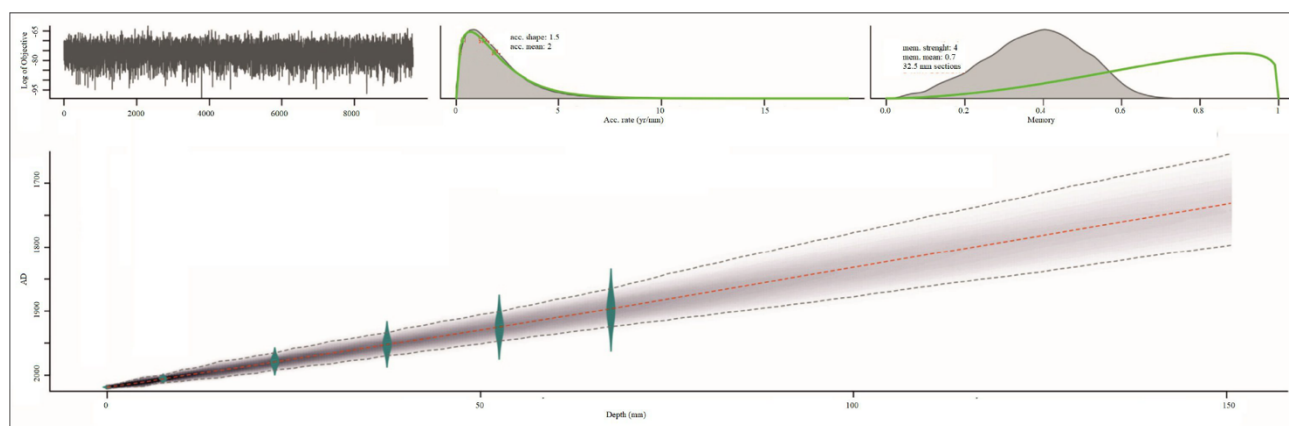| Depth (cm)	^{137}Cs (mBqg^{-1})	$^{210}Pb_{xs}$ (mBqg^{-1})	Age (CE)
0–1.5	34.3 ± 1.1	77.4 ± 1.4	2005.2 ± 2.7
1.5–3	33.0 ± 2.1	11.3 ± 0.9	1978.5 ± 8.0
3–4.5	26.2 ± 0.7	25.9 ± 1.0	1951.8 ± 13.3
4.5–6	4.6 ± 1.1	3.7 ± 0.9	1925.1 ± 18.7
6–7.5	−0.3 ± 0.6	<1	1898.4 ± 24.0

Figure 2. The age-depth model of the core G09. Top panel, from left to right: Trace plot of MCMC runs of the log-posterior distribution (left), prior (green) and posterior (shaded) distributions for accumulation rate and the memory models. Below, the age depth model is given and the 95% credible intervals for all depths are as grey shade. Green shapes indicate the distribution of the individual dates.

3.2. Lithology

A uniform textural lithology with interchanging colours between light and dark olive green colour prevailed in the Gölcük core G02 (Figure 3a). In a stratigraphical manner, light olive green fine sandy mud lasted from the deepest part of the core until 8 cm. This is followed by dark olive green fine sandy mud until 5.5 cm. From 5.5 cm, a light olive green fine sandy mud lithology similar to the first zone appeared until 4 cm. This zone is followed by dark olive green fine sandy mud until 2.4 cm. Afterwards, light olive green fine sandy mud dominated the lithology, with brief interruption by poorly sorted dark olive green sandy mud between 1.2 cm and 0.8 cm, until the topmost part of the core.

The sediment lithology of core G09 is generally comprised of interbedded intervals of fine sandy and silty mud, clayey mud and laminated layer (Figure 3b). Stratigraphically, the bottom of the core to 13.8 cm comprises of distinct dark olive green coloured fine sand and silty mud. This is followed by light olive green coloured clayey mud that prevailed until 11 cm. Afterwards, a brief and distinct light olive green fine sand and silty mud with laminated mud appeared between 11 cm and 9.5 cm. The laminated mud layers thrived and continued to dominate the lithology until 6.5 cm. From 6.5 cm to the topmost part of the core, a light olive green coloured clayey mud dominate the lithology but with interruptions of dark olive green coloured fine sand and silty mud between 6.5–5.5 cm, 4.5–3.8 cm and 2.2–1.6 cm.

In terms of sediment transport dynamics, sand and silt sediment depositions in the lithology may reflect climate change or results of mass movements. Considering the location and the geographic environment, we assume that wind is not an important sediment delivering agent but precipitation and associated mass movements may be important agents of sediment transport. No trace of abrupt event, like mass movement, is identified in the core analyses. Therefore, we assume that the presence of coarse grains (sands and silts) in the lithology is mostly controlled by climatic conditions.

3.3. Factor analysis

The results of the factor analysis of core G02 and G09 are given in Table 2 (see also Figure 4 for graphical representation). In core G02, Ca and Sr belong to F1 whereas K and Fe belong to F2. In core G09, the factor analysis revealed that the elements K, Fe and Sr belong to factor 1 (F1) and the elements Fe and Ca (which show opposite directions) belong to factor 2 (F2, Table 2).

K, Fe, and Zr are widely interpreted as indicative of terrestrial run off, whereas, Ca and Sr are indicative of endogenic carbonates (Cohen, 2003). Although Fe is an indicator of terrestrial run-off, it is also an element that is affected by redox conditions (Davison, 1993; Mackereth, 1966). The result of factor analysis in core G09; F1 elements (K, Fe, Sr) are representative of detrital materials which are delivered by terrestrial runoffs and F2 element (Ca) represents endogenic Ca precipitation. Further, the association of Sr with carbonates in core G02 and with terrestrial run off in core G09 can be related with in-lake processes or groundwater intrusions because the geological rocks surrounding the Lake Gölcük, in terms of chemical compositions, are generally uniform.
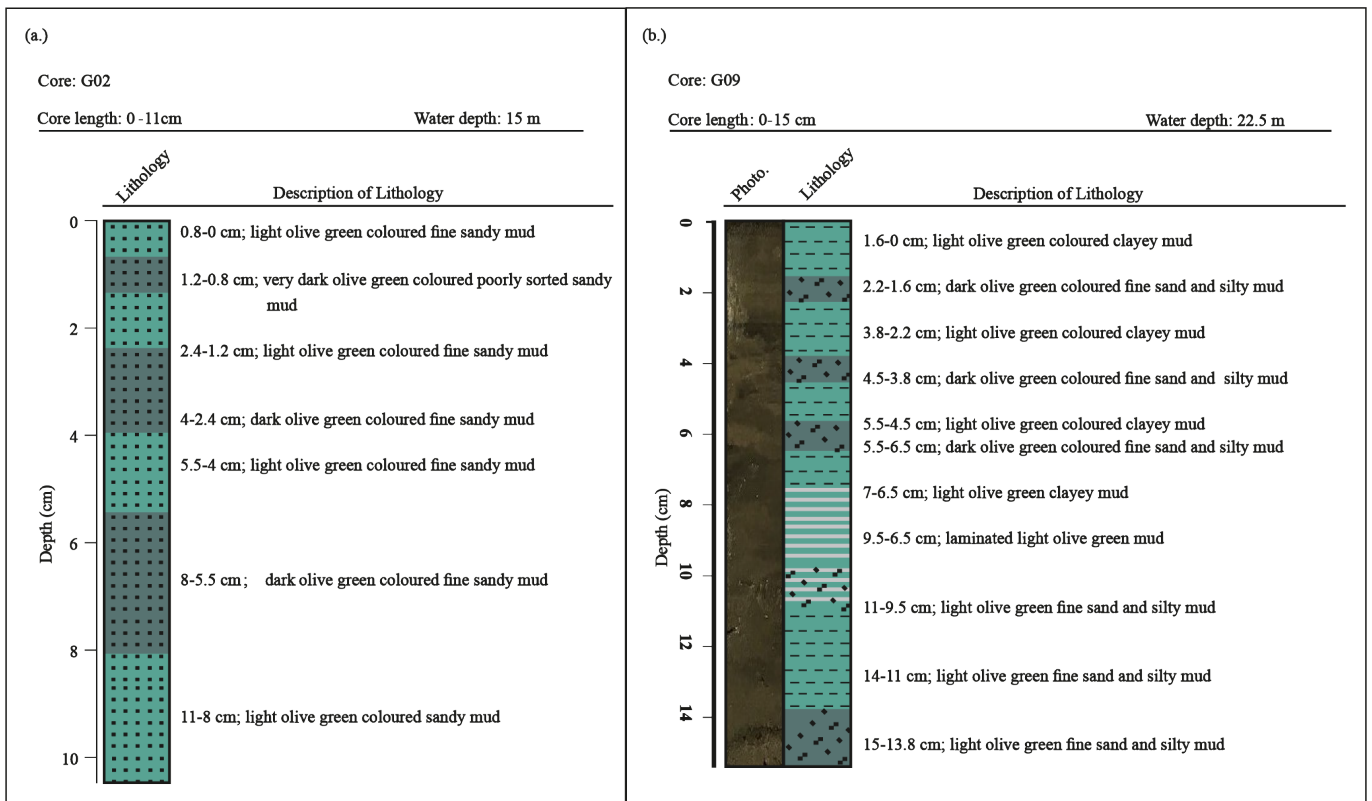

Figure 3. The lithological description of the studied cores: (a) core G02 and (b) core G09. The photograph of the core G09 is also shown at the right of the lithology.

3.4. Multiproxy results

The multiproxy results [MS, log(Ca/K), log(Sr/Ca) and lithology] of core G02 and G09 were, in visually correlated form, presented in Figure 5. The strategy for the correlation we followed are initially based on correlating the changes in geochemical data [log(Ca/K) and log(Sr/Ca)] followed by the

Table 2. The upper panel of the table shows the loadings of elemental profiles for the whole G09 and G02. Lower panel shows the sum of squared (SS) loadings, proportional variance explained by each factor and cumulative variance i.e. summation of proportional variances that show the percentage of the total variance explained by the extracted factors.

G02	Factor1	Factor2
K	−0.243	0.66
Ca	0.754	−0.164
Fe	−0.121	0.727
Sr	0.82	0.059
Zr	0.136	0.362
SS loadings	1.332	1.126
Proportion Variance	0.266	0.225
Cumulative Variance	0.266	0.492
G09	Factor1	Factor2
K	0.738	0.398
Ca	−0.023	−0.863
Fe	0.707	0.511
Sr	0.75	−0.065
Zr	0.55	0.035
SS loadings	1.909	1.17
Proportion Variance	0.382	0.234
Cumulative Variance	0.382	0.616

changes in MS (Data) in both cores. Stratigraphically, the light olive green sandy mud (11–8.5 cm) which changes to dark olive green sandy mud (8–5.5 cm), corresponds to a period with initial low values in MS and log(Sr/Ca) and high values in log(Ca/K) which changes to high values in MS and log(Sr/Ca) and low values in log(Ca/K) in core G02. Following this period, both core G02 and G09 revealed low values in MS and log(Sr/Ca) and high values in log(Ca/K) corresponding to light olive green sandy mud in core G02 (5.5–4 cm) and dark olive green fine sand and silty mud-light olive green clayey mud between 15 cm and 11 cm in core G09. Afterwards, both cores showed high values in MS and log(Sr/Ca) equivalent to dark olive green fine sandy mud in core G02 (5.5–4 cm) and fine sand and silty mud in G09 (11–9.5 cm). Subsequently, a steady increase in log(Ca/K), with two apparent interruptions indicated by high values MS and log(Sr/Ca), was observed until the top of both cores. The increase in log(Ca/K) corresponds to fine sandy mud in core G02 and light olive green clayey mud in core G09 . The core G02 lithology showed the interruption between 2.4–1.2 cm and 0.8–0 cm, whereas the interruptions were visible in the lithology of core G09 between 6.5–5.5 cm and 2.2–1.6 cm.

Magnetic susceptibility records are widely used as indicators of magnetic minerals originated from terrestrial sources, which in turn can be used to decipher wet periods (Oldfield et al., 1983; Platzman & Lund, 2019). Based on this argument, we interpret high values in MS as an increase in terrestrial run off due to precipitation. Ca/K is used as the ratio of carbonates to terrestrial run off. Carbonate precipitation changes occur with increasing temperature (Gierlowski-Kordesch, 2010), which occur during warm periods or summer periods in Lake Gölcük. Considering the interpretation of the results of our factor analysis, terrestrial run off and the fact that there are almost no $CaCO_3$ bearing units in the Lake Gölcük's surrounding, the log(Ca/K) can
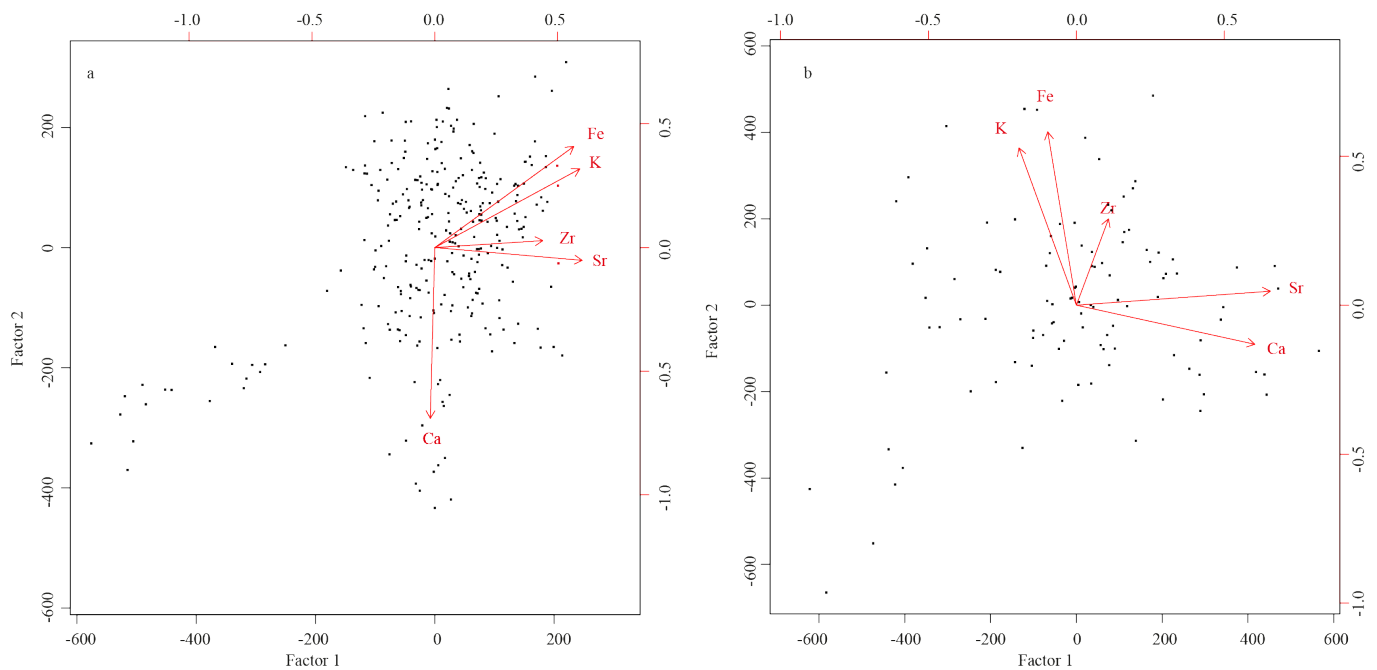

Figure 4. Biplots of results of a robust PCA of standardised K, Ca, Fe, Sr and Zr of (a) core G02 and (b) core G09.

also be used as an indicator of low terrigenous supply and high carbonate precipitation, which may also be used to infer summer temperature. Sr/Ca is generally used as an indicator of aragonite precipitation with respect to calcite which occurs in shallow water and normally an indicator of low lake water level or dry conditions (Cohen, 2003). However, it appears that log(Sr/Ca) in the lake Gölcük sedimentary records is visually opposite to log(Ca/K) and resembles the terrestrial input indicator MS, which we claim to be a proxy of carbonate precipitation and terrestrial run off due to precipitation respectively. Therefore, considering weathering related elements and terrestrial run off, log(Sr/Ca) is not a lake level proxy, unlike most previous studies' general interpretation.

To summarize, high values log(Ca/K) can be interpreted as warm summer, whereas the period with high values in MS and can be interpreted as wet period in both cores. The visual correlation in Figure 5, which is based on the changes in the geochemical and MS data, shows that the core G02 recovered from 12 m depth, has less sediment accumulation in comparison to G09, which was retrieved from 22.5 m. Similarly, based on the changes in geochemical and MS data in both cores, ~5.7 cm of core G02 is equivalent to 15 cm of core G09 (Figure 5). Considering that the lake is closed basin without surface inflows/outflows, the less sediment accumulation in core G02 can be explained by the fact that G02 is recovered from shelf, whereas G09 from deeper lake

basin. Lake basins store more sediments than slope edges. The same reason had resulted in contrasting lithology between core G02 and G09 since coarser sediments are mostly deposited in the shelf compared to the deeper basins.

3. Discussion

The present multiproxy approach based on geochemical composition [log(Ca/K) and log(Sr/Ca)], magnetic susceptibility data (MS) and lithological description permit the interpretation of the Lake Gölcük sediment cores in terms of lake catchment processes, which are influenced by climate. Since the Lake Gölcük's core G09 is the dated sediment core, the discussion section regarding the climate implications has been concentrated on this core.

Previous paleoclimate studies in the Eastern Mediterranean (including Anatolia) suggested that climate of the region is under the influence of North Atlantic Oscillation (NAO) and solar activity (Türkeş and Erlat, 2009; Luterbacher et al., 2012; Danladi and Akçer-Ön, 2018; Kushnir and Stein, 2019). The NAO has been reported to show a dipole pattern in the Mediterranean region, with NAO–(NAO+) associated with wet (warm) winter in the eastern Mediterranean and the opposite for the western (Roberts et al., 2012; Lüning et al., 2019). To unravel the climate driven mechanisms in the context of the last ~300 years, we compared the Lake Gölcük dated proxies [log(Ca/K) and MS] of core G09 with published
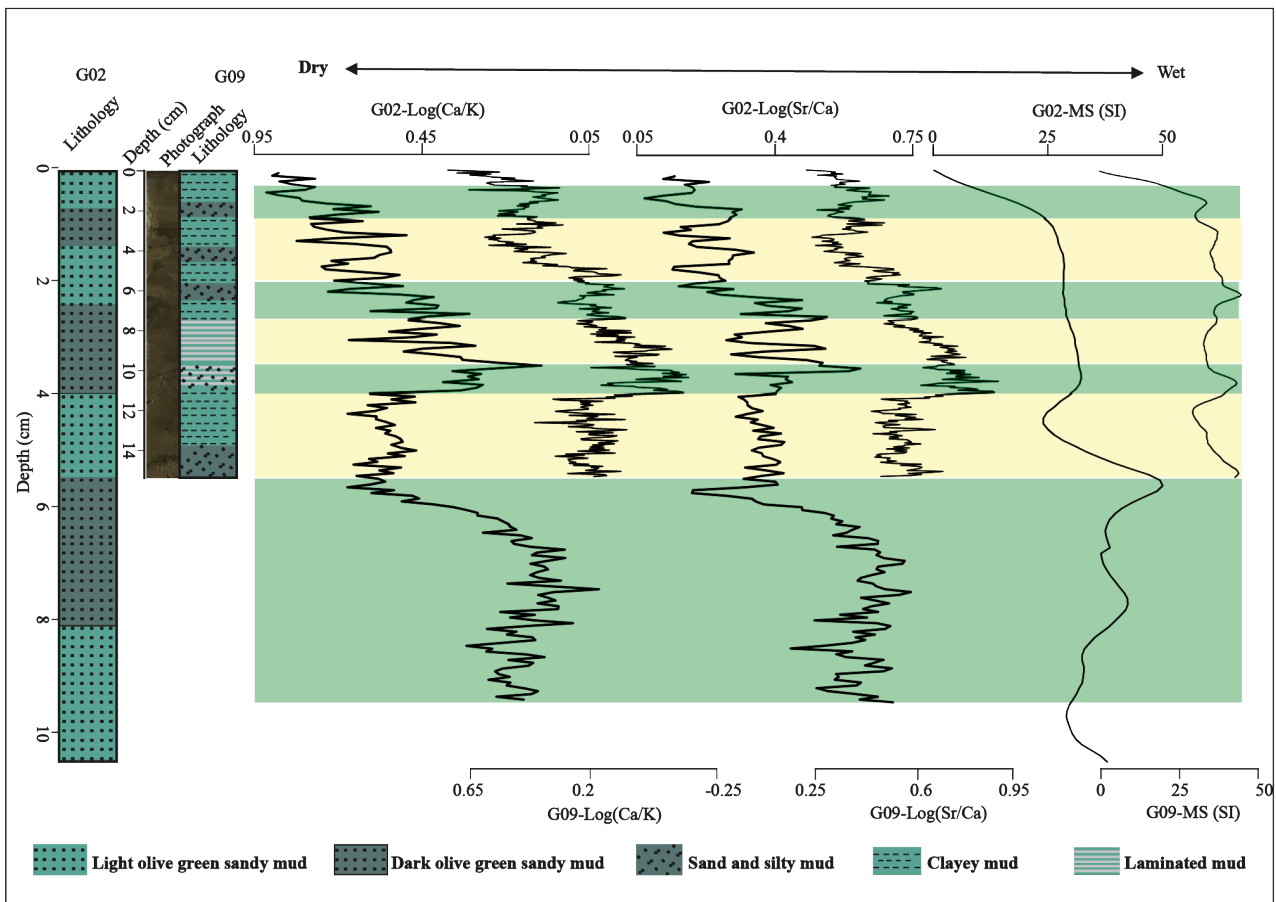

Figure 5. The visual correlation of the multiproxy results of G02 and G09 based on lithology, MS and log(Ca/K) and log(Sr/Ca). The sediment core G09 (15 cm) fits to ~5.7 cm of core G02 which is recovered from shelf.

regional climate proxy data [Lake Köyceğiz (Akçer Ön, 2017), Lake Salda (Danladi and Akçer-Ön, 2018), Lake Nar (Jones et al., 2006)), NAO reconstruction (Baker et al., 2015) and total solar irradiance reconstruction (TSI) (Delaygue and Bard, 2011) (Figure 6a)]. Additionally, for the last 120 years of data, we compared the regional precipitation (winter months; December, January, February, and March) and temperature reconstruction data (summer months; June, July, and August) with linearly detrended log(Ca/K) and MS proxies of core G09, winter NAO and yearly TSI (Figure 6b). The rationale behind choosing only winter months for precipitation

comparison relies on the fact that the region receives precipitation mainly in the winter and we assume that MS measurement substantially a proxy for detrital flux, therefore precipitation. Moreover, the summer months were chosen because these are the months the region experiences its warmest conditions and we assume that endogenic carbonate precipitation is highest through these months.

The comparison of the Lake Gölcük's log(Ca/K), a proxy for warm conditions, and MS, a proxy for wet conditions, with NAO (Figure 6a) shows that the wet periods recorded in the Lake Gölcük sedimentary records between ~ 1830(±50)–
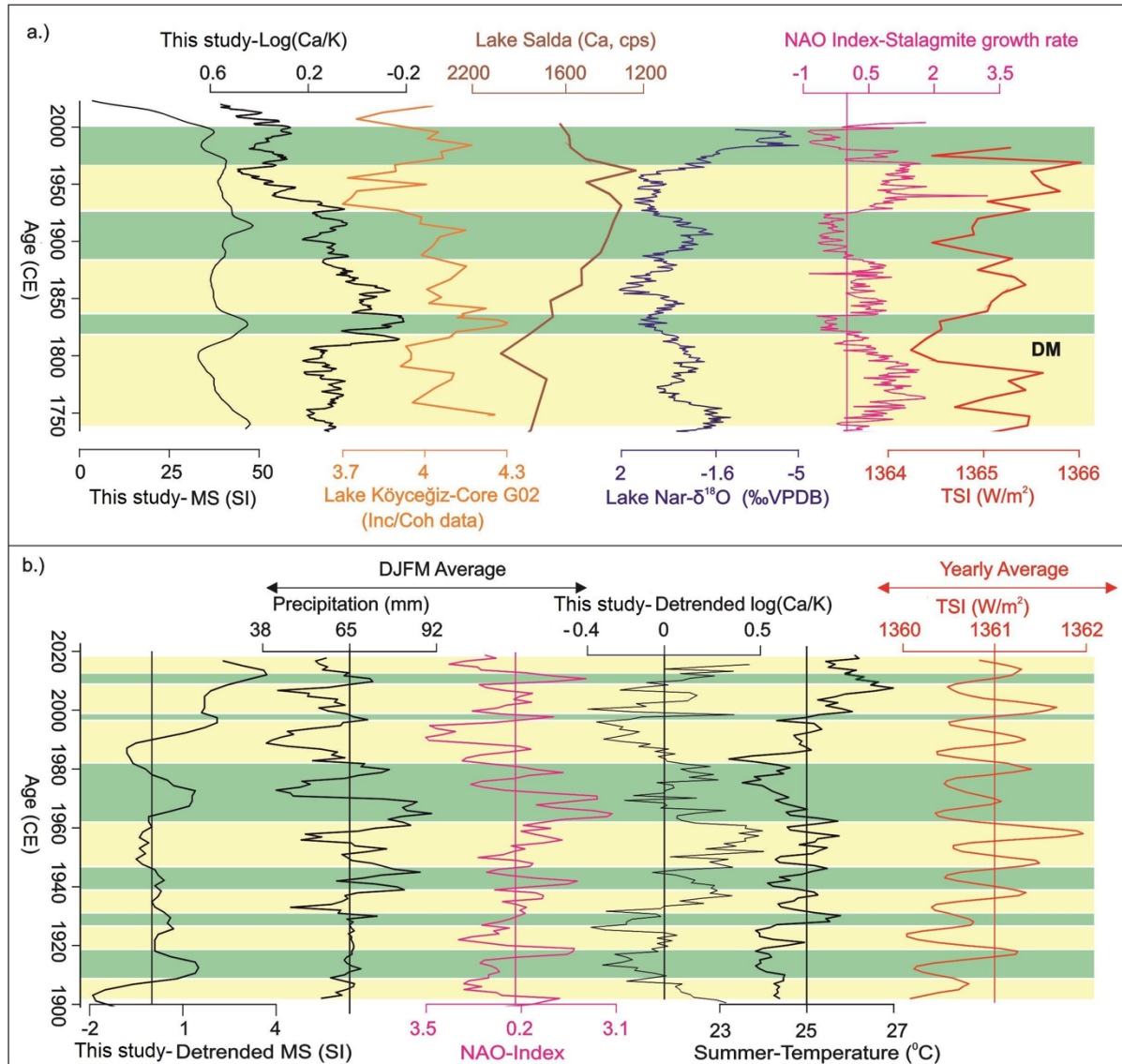

Figure 6. (a) MS and log(Ca/K) of G09 from this study correlated with climate data from Lake Köyceğiz (Inc./Coh. data; Akçer Ön, 2017), Lake Salda (Ca (cps) data; Danladi and Akçer-Ön, 2018), Lake Nar (δ¹⁸O , Jones et al., 2006), stalagmite growth rate is reconstructed NAO index (Baker et al., 2015) and reconstructed TSI (Delaygue and Bard, 2011). DM stands for Dalton Minimum. The periods with high values in MS were shaded green, while periods with high values in log(Ca/K) were shaded with beige colour. (b) A comparison of reanalysed precipitation (DJFM) and temperature (JJA) data of the Lake Gölcük region (Harris et al., 2020), Detrended MS and log(Ca/K), Winter NAO index[2] and Yearly TSI[3]. DJFM stands for December, January, February and March. Summer temperature stands for June, July and August average temperature. Green shaded regions indicate high precipitation, whereas beige shaded regions indicate high temperature.

1842(±48) CE, ~ 1885(±49)–1925(±20) CE and ~1977(±12)–2000(±6) CE are related with time of negative NAO (NAO–). On the other hand, the dry periods in the record between ~1730(±71)–1830(±50) CE, ~1842(±48)–1885(±49) CE and ~1925(±20)–1977(±12) CE are consistent with periods of positive NAO (NAO+) (Figure 6a). Likewise, excess precipitation is visually correlated with detrended MS and related with winter NAO– and vice versa (Figure 6b). This implies that excess precipitation is experienced during NAO– and vice versa. As a consequence, we claim that the NAO is an important teleconnection index affecting the precipitation of the eastern Mediterranean during the studied periods. The regional records from Lake Köyceğiz, Lake Salda, and Lake Nar were all within age uncertainties correlated with the Lake Gölcük records, thereby confirming NAO as an important component of precipitation not only for the Lake Gölcük but also for the other records (Akçer Ön, 2017; Danladi and Akçer-Ön, 2018; Jones et al., 2006). Although we compared the Lake Gölcük record with only data from lake studies, a growing body of literature related to tree rings climate reconstructions also exist (Akkemik and Aras, 2005, Touchan et al., 2005, 2007; Akkemik and Aras, 2008; Mutlu et al., 2012; Heinrich et al., 2013; Köse et al., 2017). Although these records are relatively high resolution compared to the Lake Gölcük records, we are able to delineate some similarities related with drought and wetness. For example, a May–June precipitation reconstruction from SW Anatolia (Touchan et al., 2003) recorded dry (1777, 1782, 1846, 1866, 1887, 1927 and 1928) and wet years (1753, 1771, 1783, 1816, 1877, 1896, 1901 and 1906-1907), which occasionally coincide with the periods of drier and wetter periods in the Lake Gölcük records. The differences can be related with the fact that the Lake Gölcük sedimentary records more of summer [log(Ca/K)] and winter (MS) climate variations compared to the other seasons. Similarly, in NW Anatolia, Akkemik et al. (2008) support those droughts in their May–June precipitation reconstruction. Likewise, a 250 years September–August annual tree rings reconstruction from Cyprus also recorded similar climate conditions (dry years; 1806–1824, 1915–1934 and 1986–2000), which were accordingly associated with NAO+ conditions (Griggs et al., 2014). The possible connection of the Anatolian and other EM droughts and wetness in May–August precipitation reconstruction to large scale atmospheric circulations, such as the NAO, has also been previously postulated to be non-stationary (Touchan et al., 2005).

The comparison of the Lake Gölcük records with the TSI revealed a good visual correspondence, except for a period of reduced solar activity between 1790 and 1830 CE. High (low) TSI was observed during dry (wet) periods. The good correspondence implies increase in calcium carbonate precipitation in the Lake Gölcük during increased solar activity. Accordingly, the summer temperature correlates with the detrended log(Ca/K) and were both high (low) during high (low) TSI (Figure 6b). This implies that the calcium precipitations in the Lake Gölcük occur mainly during summer and therefore the log(Ca/K) can be used as a proxy for summer temperature that results due to increase in

solar activity. On the other hand, the exceptional period of reduced solar activity falls within Dalton Minimum (1790–1830 CE) a widely discussed period of reduced solar activity (Wagner and Zorita, 2005). The Dalton Minimum is also of paleoclimate significance because it is the last phase of the Little Ice Age. The Dalton Minimum is also well registered as a dry period in the Lake Köyceğiz, Salda and Nar confirming a dry Little Ice Age in Anatolia (Jones et al., 2006; Roberts et al., 2012; Akçer Ön, 2017; Danladi and Akçer-Ön, 2018; Erginal et al., 2019). Likewise, a paleovegetation study from NE Anatolian Lake Aktaş recorded low arboreal pollen confirming dry conditions (Kılıç et al., 2018). However, the Lake Gölcük log(Ca/K) record further implies that the period during the Dalton Minimum is not only dry during winter but also cold during summer leading to elevated log(Ca/K) values. This is consistent with findings of dry and cold conditions in paleoclimate records in the East (Koutsodendris et al., 2017) and wet conditions in the West Mediterranean (Brahim et al., 2018) resulting from solar influenced hydroclimate changes.

In summary, the paleoclimate records in Anatolia appears to be affected by changes in the NAO atmospheric teleconnection and solar activity which is evident during the dry periods between ~1730(±71)–1830(±50) CE, ~1842(±48)–1885(±49) CE and ~1925(±20)–1977(±12) CE and the wet periods ~ 1830(±50)–1842(±48) CE, ~1885(±49)–1925(±20) CE and ~1977(±12)–2000(±6) CE. In a similar way, the closeness of all the compared Anatolian records in terms of precipitation/dryness tends to be mostly associated with NAO–(NAO+). The current study also confirms the previous solar-climate link studies conducted in SW Anatolian Lake Salda (Danladi and Akçer-Ön, 2018) and Lake Köyceğiz (Akçer Ön, 2017).

4. Conclusion

The multiproxy investigations (μXRF, magnetic susceptibility, lithological description and factor analysis) of two sediment cores (G02 and G09) from the Lake Gölcük (Isparta, SW Anatolia) have been presented. Using ^{210}Pb and ^{137}Cs dating methods, core G09 has been dated and the results show that the core covered the period between 1730(±71) and 2018(±3) CE.

Higher magnetic susceptibility, higher log(Sr/Ca), and dark olive green sand and silty muds revealed wet periods, whereas, higher log(Ca/K), olive green clayey mud and laminated mud suggest dry conditions in core G09. Apart from a homogeneous sandy lithology in core G02 which results from the core being recovered near the shelf, all the other proxies are interpreted similar to the core G09. We delineated the dry periods between ~1730(±71)–1830(±50) CE, ~ 1842(±48)–1885(±49) CE and ~ 1925(±20)–1977(±12) CE and ~1925(±20)–1977(±12) CE, and the wet periods ~1830(±50)–1842(±48) CE, ~ 1885(±49)–1925(±20) CE and ~ 1977(±12)–2000(±6) CE.

The dated Lake Gölcük record of core G09 have been compared with published regional data, NAO and TSI. All the wet periods identified in the Lake Gölcük records are correlated with periods of NAO– and low solar activity, whereas, the dry periods with the exception of the Dalton

Minimum, are correlated with NAO+ and high solar activity. The Dalton Minimum, which is a period of low solar activity (1790–1830 CE) and the last phase of the Little Ice Age, has been observed as a dry period in the Lake Gölcük record. The comparisons between the winter precipitations and the summer temperatures with the detrended MS and log(Ca/K) data derived from the sediment core G02 suggest a relation between the NAO– on the precipitation regime in the region. Also, the sediment log(Ca/K) data show a positive correlation with the periods of increased temperature and increased solar activity. Furthermore, this study reveals the high potential of the Lake Gölcük sedimentary records in terms of paleoclimate reconstructions that may cover longer times scales such as the Holocene and Quaternary.

References

Akçer Ön S (2017). Küçük Buz Çağı'nda Güneş etkisine bağlı iklim değişimleri: Köyceğiz Gölü çökel kayıtları (GB Anadolu). Türkiye Jeoloji Bülteni 60 (4): 569-588 (in Turkish) doi: 10.25288/tjb.370616

Akkemik Ü, Aras A (2005). Reconstruction (1689-1994 AD) of April-August precipitation in the southern part of central Turkey. International Journal of Climatology 25 (4): 537-548. doi: 10.1002/joc.1145

Akkemik Ü, D'Arrigo R, Cherubini P, Köse N, Jacoby GC (2008). Tree-ring reconstructions of precipitation and streamflow for north-western Turkey. International Journal of Climatology. doi: 10.1002/joc.1522

Appleby PG (2002). Chronostratigraphic techniques in recent sediments. In: Last WM, Smol JP (editors). Tracking Environmental Change Using Lake Sediments. Developments in Paleoenvironmental Research. Vol. 1. Dordrecht, Netherlands: Springer, pp. 171-203.

Baker AC, Hellstrom J, Kelly BFJ, Mariethoz G, Trouet V (2015). A composite annual-resolution stalagmite record of North Atlantic climate over the last three millennia. Scientific Reports. doi: 10.1038/srep10307

Brahim YA, Wassenburg JA, Cruz FW, Sifeddine A, Scholz D et al. (2018). Multi-decadal to centennial hydro-climate variability and linkage to solar forcing in the Western Mediterranean during the last 1000 years. Scientific Reports 8 (1): 1-8. doi: 10.1038/s41598-018-35498-x

Blaauw M, Christen JA (2011). Flexible paleoclimate age-depth models using an autoregressive gamma process. Bayesian Analysis 6: 457-474. doi: 10.1214/ba/1339616472

Canpolat E (2015). Gölcük volkanik alanının jeomorfolojisi, Isparta - Türkiye. Coğrafya Dergisi 32: 62-82 (in Turkish).

Cengiz O, Sener E, Yagmurlu F (2006). A satellite image approach to the study of lineaments, circular structures and regional geology in the Golcuk Crater district and its environs (Isparta, SW Turkey). Journal of Asian Earth Sciences. doi: 10.1016/j.jseaes.2005.02.005

Cohen SA (2003). Paleolimnology: The History and Evolution of Lake Systems. Oxford, UK: Oxford University Press. doi: 10.1669/0883-1351(2004)019<0184:br>2.0.co;2

Cook BI, Anchukaitis KJ, Touchan R, Meko DM, Cook ER (2016). Spatiotemporal drought variability in the mediterranean over the last 900 years. Journal of Geophysical Research. doi: 10.1002/2015JD023929

Croudace IW, Löwemark L, Tjallingii R, Zolitschka B (2019). Current perspectives on the capabilities of high resolution XRF core scanners. Quaternary International. doi: 10.1016/j.quaint.2019.04.002

Croudace IW, Rindby A, Rothwell RG (2006). ITRAX: Description and evaluation of a new multi-function X-ray core scanner. Geological Society Special Publication. doi: 10.1144/GSL.SP.2006.267.01.04

Danladi, IB, Akçer-Ön S (2018). Solar forcing and climate variability during the past millennium as recorded in a high altitude lake: Lake Salda (SW Anatolia). Quaternary International 486. doi: 10.1016/j.quaint.2017.08.068

Davison W (1993). Iron and manganese in lakes. Earth Science Reviews. doi: 10.1016/0012-8252(93)90029-7

Delaygue G, Bard E (2011). An Antarctic view of Beryllium-10 and solar activity for the past millennium. Climate Dynamics 36 (11-12): 2201-2218. doi: 10.1007/s00382-010-0795-1

Devlet Su İşleri Genel Müdürlüğü (DSİ) (1978). Gölcük Gölü Batimetri Haritası. Ankara, Turkey: DSİ (in Turkish).

Erginal AE, Selim HH, Karabiyikoglu M (2019). Multi-proxy sedimentary records of dry-wet climate cycles during the last 2 ka from lake Çıldır, East Anatolian Plateau, Turkey 1001(1170627). doi: 10.4461/GFDQ.2019.42.5

Filzmoser P, Hron K, Reimann C, Garrett R (2009). Robust factor analysis for compositional data. Computers & Geosciences 35 (9): 1854-1861. doi: 10.1016/j.cageo.2008.12.005

Filzmoser P, Hron K, Templ M (2018). Applied compositional data analysis. Switzerland: Springer Nature. doi: 10.1007/978-3-319-96422-5

Gierlowski-Kordesch EH (2010). Lacustrine Carbonates. In: Alonso-Zarza AM, Tanner LH (editors). Carbonates in Continental Settings: Facies, Environments, and Processes. Vol. 61. Amsterdam, Netherlands: Elsevier.

Giorgi F (2006). Climate change hot-spots. Geophysical Research Letters. doi: 10.1029/2006GL025734

Griggs C, Pearson C, Manning SW, Lorentzen B (2014). A 250-year annual precipitation reconstruction and drought assessment for Cyprus from Pinus brutia Ten. tree-rings. International Journal of Climatology 34 (8): 2702-2714. doi: 10.1002/joc.3869

Heinrich I, Touchan R, Dorado Liñán I, Vos H, Helle G (2013). Winter-to-spring temperature dynamics in Turkey derived from tree rings since AD 1125. Climate Dynamics 41: 1685-1701. doi: 10.1007/s00382-013-1702-3

Hurrell JW (1995). Decadal trends in the North Atlantic oscillation: regional temperatures and precipitation. Science 269 (5224): 676-679. doi: 10.1126/science.269.5224.676

Japoshvili G, Kaya M, Aslan B, Karaca I (2017). Coleoptera diversity and abundance in Golcuk Natural Park, in Isparta, Turkey. Entomologia Hellenica 18: 47-55. doi: 10.12681/eh.11607

Japoshvili G, Çelik H, Aslan B, Karaca I (2010). Hymenopteran diversity and abundance in Gölcük Natural Park in Isparta, Turkey. Turkiye Entomoloji Dergisi 34 (4): 435-446. doi: 10.16970/ted.19549

Jones MD, Roberts CN, Leng M, Türkeş M (2006). A high-resolution late Holocene lake isotope record from Turkey and links to North Atlantic and monsoon climate. Geology 34 (5): 361-364. doi: 10.1130/G22407.1

Kahya E (2011). The impacts of NAO on the hydrology of the Eastern Mediterranean. In: Vicente-Serrano S, Trigo R (editors). Hydrological, Socioeconomic and Ecological Impacts of the North Atlantic Oscillation in the Mediterranean Region. Advances in Global Change Research. Vol. 46. Dordrecht, Netherlands: Springer. doi: 10.1007/978-94-007-1372-7_5

Kılıç NK, Caner H, Erginal AE, Ersin S, Selim HH et al. (2018). Environmental changes based on multi-proxy analysis of core sediments in Lake Aktaş Turkey: Preliminary results. Quaternary International. doi: 10.1016/j.quaint.2018.02.004

Köse N, Tuncay GH, Harley G, Guiot J (2017). Spring temperature variability over Turkey since 1800 CE reconstructed from a broad network of tree-ring data. Climate of the Past 13 (1): 1-15. doi: 10.5194/cp-13-1-2017

Koutsodendris A, Brauer A, Reed JM, Plessen B, Friedrich O et al. (2017). Climate variability in SE Europe since 1450 AD based on a varved sediment record from Etoliko Lagoon (Western Greece). Quaternary Science Reviews. doi: 10.1016/j.quascirev.2017.01.010

Kushnir Y, Stein M (2019). Medieval climate in the Eastern Mediterranean: Instability and evidence of solar forcing. Atmosphere. doi: 10.3390/atmos10010029

Kutiel H, Maheras P, Türkeş M, Paz S (2002). North Sea - Caspian Pattern (NCP) - An upper level atmospheric teleconnection affecting the eastern Mediterranean - Implications on the regional climate. Theoretical and Applied Climatology 72 (3-4): 173-192. doi: 10.1007/s00704-002-0674-8

Lelieveld J, Hadjinicolaou P, Kostopoulou E, Chenoweth J, El Maayar M et al. (2012). Climate change and impacts in the Eastern Mediterranean and the Middle East. Climatic Change. doi: 10.1007/s10584-012-0418-4

Lüning S, Schulte L, Garcés-Pastor S, Danladi IB, Gałka M (2019). The Medieval Climate Anomaly in the Mediterranean Region. Paleoceanography and Paleoclimatology. doi: 10.1029/2019PA003734

Luterbacher J, García-Herrera R, Akcer-On S, Allan R, Alvarez-Castro MC et al. (2012). A review of 2000 years of paleoclimatic evidence in the mediterranean. In: Lionello P (editor). The Climate of the Mediterranean Region: From the Past to the Future. London, UK: Elsevier. doi: 10.1016/B978-0-12-416042-2.00002-1

Mackereth FJH (1966). Some chemical observations on post-glacial lake sediments. Philosophical Transactions of the Royal Society of London Series B, Biological Sciences 250 (765). doi: 10.1098/rstb.1966.0001

Martín-Puertas C, Valero-Garcés BL, Mata MP, Moreno A, Giral S et al. (2009). Geochemical processes in a Mediterranean Lake: a high-resolution study of the last 4,000 years in Zoñar Lake, southern Spain. Paleolimnology 46: 405-421. doi: 10.1007/s10933-009-9373-0

Mutlu H, Köse N, Akkemik Ü, Aral D, Kaya A et al. (2012). Environmental and climatic signals from stable isotopes in Anatolian tree rings, Turkey. Regional Environmental Change 12 (3): 559-570. doi: 10.1007/s10113-011-0273-2

Oldfield F, Barnosky C, Leopold EB, Smith JP (1983). Mineral magnetic studies of lake sediments - a brief review. Hydrobiologia. doi: 10.1007/BF00028425

Öztürk Y (2017). Bird diversity and conservation status in Isparta province (Turkey). Journal of Environmental Biology. doi: 10.22438/jeb/38/5(SI)/GM-14

R Core Team (2020). R: A language and environment for statistical computing. Vienna, Austria: R Foundation for Statistical Computing.

Reimann C, Filzmoser P, Garrett RG, Dutter R (2008). Principal component analysis (PCA) and factor analysis (FA). In: Statistical Data Analysis Explained. Hoboken, NJ, USA: John Wiley & Sons. doi: 10.1002/9780470987605.ch14

Platzman ES, Lund SP (2019). High-resolution environmental magnetic study of a Holocene sedimentary record from Zaca Lake, California. Holocene. doi: 10.1177/0959683618804636

Roberts N, Moreno A, Valero-Garcés BL, Corella JP, Jones M et al. (2012). Palaeolimnological evidence for an east-west climate see-saw in the Mediterranean since AD 900. Global and Planetary Change 84-85: 23-34. doi: 10.1016/j.gloplacha.2011.11.002

Schmidt S, Howa, Diallo A, Martí J, Cremer M et al. (2014). Recent sediment transport and deposition in the Cap-Ferret Canyon, South-East margin of Bay of Biscay. Deep-Sea Research Part II: Topical Studies in Oceanography. doi: 10.1016/j.dsr2.2013.06.004

Stocker TF, Qin D, Plattner GK, Tignor MMB, Allen SK et al. (2013). Climate Change 2013 the Physical Science Basis: Working Group I Contribution to the Fifth Assessment Report of the Intergovernmental Panel on Climate Change. New York, NY, USA: Cambridge University Press. doi: 10.1017/CBO9781107415324

Touchan R, Akkemik Ü, Hughes MK, Erkan N (2007). May-June precipitation reconstruction of southwestern Anatolia, Turkey during the last 900 years from tree rings. Quaternary Research 68 (2): 196-202. doi: 10.1016/j.yqres.2007.07.001

Touchan R, Garfin GM, Meko DM, Funkhouser G, Erkan N et al. (2003). Preliminary reconstructions of spring precipitation in Southwestern Turkey from tree-ring width. International Journal of Climatology. doi: 10.1002/joc.850

Touchan R, Xoplaki E, Funkhouser G, Luterbacher J, Hughes MK et al. (2005). Reconstructions of spring/summer precipitation for the Eastern Mediterranean from tree-ring widths and its connection to large-scale atmospheric circulation. Climate Dynamics 25 (1): 75-98. doi: 10.1007/s00382-005-0016-5

Türkeş M, Erlat E (2009). Winter mean temperature variability in Turkey associated with the North Atlantic Oscillation. Meteorology and Atmospheric Physics 105 (3-4): 211-225. doi: 10.1007/s00703-009-0046-3

Wagner S, Zorita E (2005). The influence of volcanic, solar and CO2 forcing on the temperatures in the Dalton Minimum (1790-1830): a model study. Climate Dynamics. doi: 10.1007/s00382-005-0029-0

Weber ME, Niessen F, Kuhn G, Wiedicke M (1996). Calibration and application of marine sedimentary physical properties using a multi-sensor core logger. Marine Geology 136 (3-4): 151-172. doi: 10.1016/S0025-3227(96)00071-0

Weltje G, Tjallingii R (2008). Calibration of XRF core scanners for quantitative geochemical logging of sediment cores: theory and application. Earth and Planetary Science Letters 274 (3-4): 423-438. doi: 10.1016/j.epsl.2008.07.054

Yavuz M, Çobanoğlu G (2018). Lichen diversity of Gölcük Nature Park (Isparta), including new records for Turkey. Muzeul Olteniei Craiova. Oltenia. Studii Şi Comunicări. Ştiinţele Naturii 34 (2): 57-66.